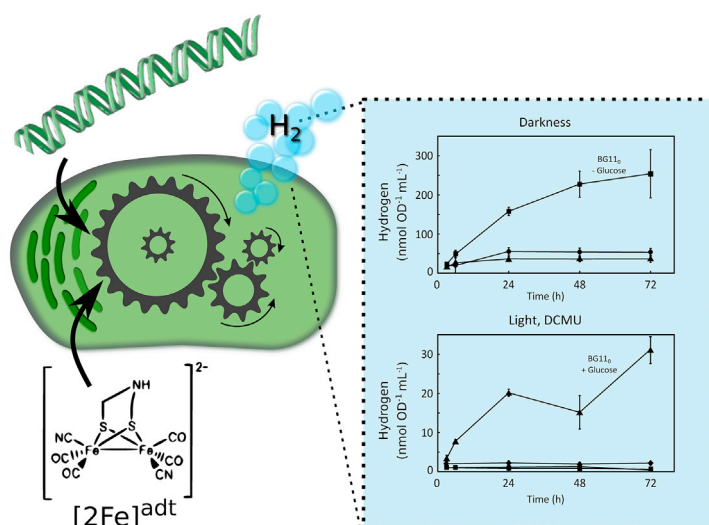


# Article

# Semisynthetic [FeFe]-hydrogenase with stable expression and H<sub>2</sub> production capacity in a photosynthetic microbe



[FeFe]-hydrogenases are hydrogen (H<sub>2</sub>)-producing metalloenzymes with excellent catalytic capacities. Photosynthetic cyanobacteria are promising chassis for large-scale H<sub>2</sub> production due to their fast growth and minimalistic substrate requirement. Wegelius et al. use artificial activation to enable sustainable *in vivo* H<sub>2</sub> production from newly discovered [FeFe]-hydrogenases expressed in a unicellular cyanobacterium.

Adam Wegelius, Henrik Land, Gustav Berggren, Peter Lindblad

peter.lindblad@kemi.uu.se

## HIGHLIGHTS

Artificial activation of newly discovered [FeFe]-hydrogenases expressed in cyanobacteria

Stable expression and significant H<sub>2</sub> production under different environmental conditions

Activated, semisynthetic [FeFe]-hydrogenase remains functional *in vivo* for several days

## Article

Semisynthetic [FeFe]-hydrogenase with stable expression and H<sub>2</sub> production capacity in a photosynthetic microbeAdam Wegelius,<sup>1</sup> Henrik Land,<sup>2,3</sup> Gustav Berggren,<sup>2,5</sup> and Peter Lindblad<sup>1,4,6,\*</sup>

## SUMMARY

Hydrogen (H<sub>2</sub>) is a promising future chemical energy carrier and feedstock with several renewable production options, including electrolyzers and biological/bioinspired systems. The top H<sub>2</sub> producers in nature are [FeFe]-hydrogenases, high turnover metalloenzymes with a complex maturation process that can be circumvented by artificial synthetic activation. Here, we report the expression and activation of group A and D [FeFe]-hydrogenases in a photosynthetic host organism, the unicellular cyanobacterium *Synechocystis* PCC 6803. The hydrogenase from *Solobacterium moorei* (group A) facilitates high *in vivo* H<sub>2</sub> production from purely photoautotrophically generated substrates and unmistakably links to the metabolism of the photosynthetic host. Cells harboring the non-native, semisynthetic enzyme retain their H<sub>2</sub> production capacity for several days after synthetic activation. This work expands both the number and the diversity of [FeFe]-hydrogenases examined in a photosynthetic background and provides important insights for future investigations into the development and understanding of biological and biohybrid H<sub>2</sub> production systems.

## INTRODUCTION

Molecular hydrogen (H<sub>2</sub>) can be used as a clean fuel or chemical feedstock and will be vital in the search for alternatives to fossil carbon sources. Although almost all available H<sub>2</sub> gas still is derived from fossil sources, many alternatives are under investigation and/or development. Renewable, so-called green, H<sub>2</sub> is generated in electrolyzers when using renewable green electricity or, in similarity with fermentative biogas production, generated by microbial fermentation.<sup>1,2</sup> Cyanobacteria are a phylum of photosynthetic microbes, some of which display the natural production of H<sub>2</sub> gas catalyzed by a bidirectional [NiFe]-hydrogenase or by nitrogenase during N<sub>2</sub> fixation.<sup>3</sup> This native production of a ready-to-use fuel compound, using only light as energy source and water as electron donor, has understandably attracted a lot of attention in the field of biofuel research. Consequently, several cyanobacterial strains have been explored and engineered in the pursuit of efficient H<sub>2</sub> producers.<sup>3–6</sup>

Biological H<sub>2</sub> production systems remain most promising, even in light of the recent development of artificial systems,<sup>7,8</sup> due to, for example, facile scalability and independence of rare metals. However, to become truly viable, efficiencies and stability need to be significantly improved. A possible strategy to advance biological H<sub>2</sub> production is the utilization of [FeFe]-hydrogenases, nature's most formidable H<sub>2</sub> producers. These hydrogenases, found in certain anaerobic bacteria and green algae,

<sup>1</sup>Microbial Chemistry, Department of Chemistry-Ångström, Uppsala University, Uppsala, Box-523, 751 20, Sweden

<sup>2</sup>Molecular Biomimetics, Department of Chemistry-Ångström, Uppsala University, Uppsala, Box-523, 751 20, Sweden

<sup>3</sup>Twitter: @henrikland1

<sup>4</sup>Twitter: @LindbladPeter

<sup>5</sup>Twitter: @berggrenlab

<sup>6</sup>Lead contact

\*Correspondence: [peter.lindblad@kemi.uu.se](mailto:peter.lindblad@kemi.uu.se)  
<https://doi.org/10.1016/j.xcrp.2021.100376>



are known for their unmatched  $H_2$  production capacity and high turnover numbers.<sup>9–11</sup> The active site of [FeFe]-hydrogenase contains a cofactor, known as the H-cluster, consisting of a [4Fe-4S] cluster connected to a diiron subcluster via a cysteine bridge. [FeFe]-hydrogenases are, in their native hosts, always accompanied by a maturation machinery (HydEFG) that performs the assembly and insertion of the diiron subcluster into the active site.<sup>12</sup> The expression of an [FeFe]-hydrogenase in a host cell lacking a functional maturation machinery will result in an unmaturing, inactive, *apo*-enzyme with a partially formed H-cluster in which the diiron subcluster is missing. This has long been an inconvenience for both *in vivo* and *in vitro* biotechnological applications and creative workarounds have been developed, using both *in vitro* and recombinant *in vivo* maturation.<sup>13,14</sup> In the filamentous cyanobacterium *Nostoc* PCC 7120, expression of a group A [FeFe]-hydrogenase from *Clostridium acetobutylicum* and its corresponding maturation machinery, resulted in phototrophic  $H_2$  production.<sup>15</sup> Alternatively, a direct *in vitro* maturation of purified *apo*-enzyme by a synthetic diiron subcluster mimic also results in an active enzyme.<sup>16,17</sup>

Recently, it was discovered that a synthetic subcluster mimic could be used to activate an unmaturing [FeFe]-hydrogenase from the unicellular green algae *Chlamydomonas reinhardtii* (*Cr* HydA1) directly in living cells of the model bacterium *Escherichia coli*.<sup>18</sup> We later proved that the *in vivo* strategy worked also in cyanobacteria, by synthetically activating the *Cr* HydA1 expressed in *Synechocystis* PCC 6803.<sup>19</sup> The semisynthetic enzyme accepted internally produced reduction equivalents and produced  $H_2$  under a number of environmental conditions, in which both the fastest and most long-lived production was observed under  $N_2$  deprivation in absence of light.<sup>19</sup>

Based on *in vivo* activation work in *E. coli*<sup>18</sup> and the recent discovery that the cofactor of the semisynthetic enzyme can be monitored *in vivo* by electron paramagnetic resonance (EPR) spectroscopy,<sup>20</sup> Land et al.<sup>21</sup> developed a screening method for the rapid identification and characterization of new [FeFe]-hydrogenases without the need for protein purification and specialized expression environments. In the same study, two novel [FeFe]-hydrogenases, *Sm* HydA from *Solobacterium moorei* (a strictly anaerobic bacterium originally isolated from human feces<sup>22</sup>) and *Tam* HydS from *Thermoanaerobacter mathranii* (a thermophilic spore-forming eubacterium isolated from hot springs<sup>23</sup>), were discovered and analyzed further.

[FeFe]-hydrogenase is a diverse family of enzymes that divide into four groups (A–D) that are further divided into a plethora of subclasses with a wide variety of domain architectures that influence their respective functions.<sup>24–27</sup> *Sm* HydA belongs to group A, subclass M2, and is therefore a so-called prototypical [FeFe]-hydrogenase. Group A enzymes are known for their high activity, and a well-studied example from the same subclass is the [FeFe]-hydrogenase from *Megasphaera elsdenii*.<sup>28,29</sup> *Sm* HydA has previously only been partially characterized, but it shows indications of a high specific activity.<sup>21</sup> On the other side of the [FeFe]-hydrogenase spectrum, *Tam* HydS, belonging to group D and subclass M2e, is a putative sensory enzyme with low recorded activities in *E. coli* as well as *in vitro*.<sup>21,30</sup> Exploration and application of a broad spectrum of different [FeFe]-hydrogenases will be key in unlocking the true potential of this enzyme family.

In the present work, we use artificial activation to show  $H_2$  production from the two newly discovered [FeFe]-hydrogenases, *Sm* HydA from *Solobacterium moorei* and *Tam* HydS from *Thermoanaerobacter mathranii*, in cells of a photosynthetic

prokaryote, the cyanobacterium *Synechocystis*. This expands the number and variety of hydrogenases characterized in cyanobacteria and highlights differences in performance when used in a photosynthetic context. We could detect *in vivo* H<sub>2</sub>-evolution activity from both enzymes after synthetic activation by the diiron sub-cluster mimic. *Synechocystis* cells carrying the activated *Sm* HydA exhibits clear H<sub>2</sub> production under different environmental conditions, and the semisynthetic enzyme remains stable *in vivo* for several days.

## RESULTS AND DISCUSSION

### Expression of *Sm* HydA and *Tam* HydS in *Synechocystis*

We expressed two novel FeFe-hydrogenases, *Sm* HydA (Table S1) from *Solobacterium moorei* and *Tam* HydS (Table S1) from *Thermoanaerobacter mathranii*, in a hydrogenase-deficient ( $\Delta$ hoxYH) strain of the unicellular cyanobacterium *Synechocystis* PCC 6803 (*Synechocystis*  $\Delta$ hox), resulting in strains *Synechocystis*  $\Delta$ hox *SmhydA* and *Synechocystis*  $\Delta$ hox *TamhydS*. The complete absence of hydrogenase activity in the background strain enables reliable and exact *in vivo* activity assessments of the heterologously expressed hydrogenases.

### Semisynthetic hydrogenase capable of *in vivo* H<sub>2</sub> production in a photosynthetic host

After a period of photoautotrophic growth, cultures of the 2 recombinant strains were made anaerobic and incubated with 100  $\mu$ g (50  $\mu$ g/mL, 78  $\mu$ M) synthetic mimic of the diiron subcluster [Fe<sub>2</sub>(adt)(CO)<sub>4</sub>(CN)<sub>2</sub>]<sup>2-</sup> (from here, [2Fe]<sup>adt</sup>, adt = -SCH<sub>2</sub>NHCH<sub>2</sub>S-). H<sub>2</sub> production was monitored under dark conditions in cultivation media with and without added nitrate (BG11 and BG11<sub>0</sub>, respectively) and/or glucose. No production of H<sub>2</sub> could be detected from *Synechocystis*  $\Delta$ hox *TamhydS* in any of the four tested dark conditions, but the *Synechocystis*  $\Delta$ hox *SmhydA* strain showed distinct H<sub>2</sub> accumulation in both of the nitrate-deprived conditions, and in BG11 with the addition of glucose, already after 3 h. Accumulated H<sub>2</sub> from *Synechocystis*  $\Delta$ hox *SmhydA* after activation and 24 h of dark incubation in different medium compositions can be seen in Figure 1A. The highest H<sub>2</sub> production was observed in N<sub>2</sub>-deprived conditions without glucose supplementation, in which 158 ( $\pm$ 11) nmol H<sub>2</sub> optical density at 750nm (OD)<sup>-1</sup> mL<sup>-1</sup> was measured after 24 h. Glucose-supplemented cell cultures in BG11 and BG11<sub>0</sub> had produced less than half at the same time point, 56 ( $\pm$ 9) and 36 ( $\pm$ 7) nmol H<sub>2</sub> OD<sup>-1</sup> mL<sup>-1</sup>, respectively. No accumulation of H<sub>2</sub> could be observed for *Synechocystis*  $\Delta$ hox *SmhydA* in BG11 without glucose. As expected, we could not, under any condition, detect H<sub>2</sub> production from cell cultures in which no [2Fe]<sup>adt</sup> were added. Likewise, no H<sub>2</sub> production was detected when the background strain *Synechocystis*  $\Delta$ hox was incubated with [2Fe]<sup>adt</sup>. Increased Hox-dependent H<sub>2</sub> production in nitrate-deprived conditions has been reported from *Synechocystis* wild-type cell cultures during dark fermentation.<sup>31</sup> This is due to the arrest of the reductant demanding nitrate assimilation pathway.<sup>32</sup> The observation that *Sm* HydA and Hox catalyzed H<sub>2</sub> production follows the same trend suggests that the native and the recombinant subclass M2 enzyme connects to the cellular metabolism in a comparable way.

Time profiles of the H<sub>2</sub> accumulation in darkness (Figure 1B) reveal that no further net production occurs after 24 h (Figure 1B). Conversely, in BG11<sub>0</sub> without glucose, H<sub>2</sub> production continues beyond 24 h, reaching above 250 nmol H<sub>2</sub> OD<sup>-1</sup> mL<sup>-1</sup> at the end of the experiment, the highest recorded level in this work (Figure 1B). This is considerable production, and the H<sub>2</sub> contents in the sample vials were >2%.

To facilitate anoxygenic photohydrogen production, *Synechocystis*  $\Delta$ hox *SmhydA* was treated as above with [2Fe]<sup>adt</sup> and incubated under continuous illumination

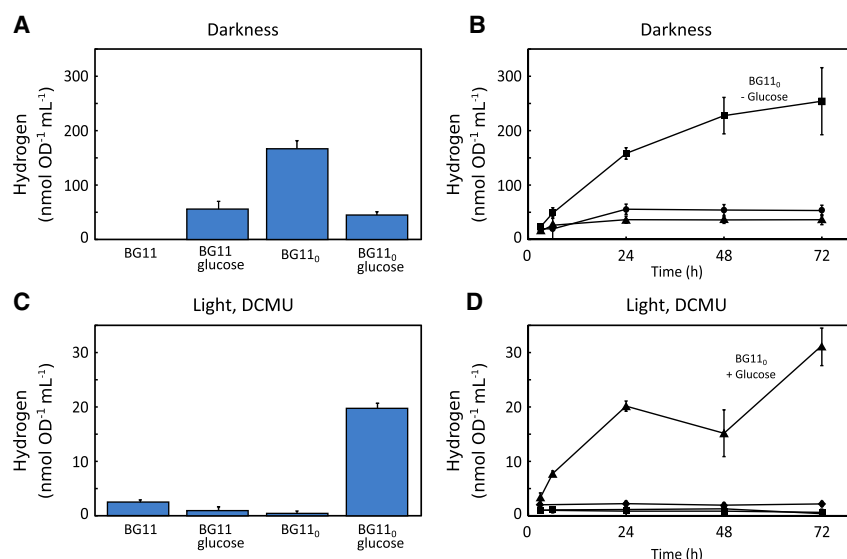


**Figure 1. In vivo H<sub>2</sub> production from synthetically activated *Solobacterium* HydA in *Synechocystis***

Accumulated H<sub>2</sub> production by *Synechocystis* PCC 6803  $\Delta$ hox harboring a synthetically activated *Sm* HydA.

(A and C) Accumulated H<sub>2</sub> 24 h after synthetic activation and incubation with different media composition in (A) darkness and (C) light with DCMU inhibition.

(B and D) Time profiles of H<sub>2</sub> accumulation in (B) darkness and (D) light with DCMU inhibition during incubation in BG11 (diamonds), BG11 with glucose (circles), BG11<sub>0</sub> (squares), and BG11 with glucose (triangles).

Figures display nanomoles of accumulated H<sub>2</sub> gas/mL culture, normalized to optical density (OD<sub>750</sub> nm). Data points represent means of 2–6 individual experiments and error bars depict SDs.

(80  $\mu$ mol photons m<sup>-2</sup> s<sup>-1</sup>) with photosystem II (PSII) inhibition by DCMU (3-(3,4-dichlorophenyl)-1,1-dimethylurea). The highest H<sub>2</sub> accumulation under these conditions was found in N<sub>2</sub>-deprived conditions with glucose (Figure 1C). 24 h after incubation with [2Fe]<sup>ad</sup>, 20 ( $\pm$  1) nmol H<sub>2</sub> OD<sup>-1</sup> mL<sup>-1</sup> could be detected in the head-space of the sample vials, similar to the content in the corresponding condition in darkness. In the other 3 conditions (BG11 with/without glucose and BG11<sub>0</sub> without glucose), the accumulated H<sub>2</sub> levels were 10 times lower or even less in light with DCMU, compared to the corresponding dark conditions. Thus, we can conclude that if any photohydrogen production via PSI is facilitated by the semisynthetic hydrogenase under continuous light, it is of minor importance. No O<sub>2</sub> evolution was observed from cultures under light with DCMU inhibition, ruling out inactivation by O<sub>2</sub> as the cause for the limited production. The addition of DCMU to darkness samples did not have any negative effect on H<sub>2</sub> production.

Time profiles of H<sub>2</sub> accumulation under light (Figure 1D) shows that the only tested growth medium that facilitates any significant H<sub>2</sub> production after 3 h is glucose-supplemented BG11<sub>0</sub>. The apparent drop in accumulated H<sub>2</sub> at 48 h in BG11<sub>0</sub> with glucose could indicate H<sub>2</sub> oxidation activity of *Sm* HydA under these conditions. Unfortunately, our data do not let us conclude whether this presumed consumption is substantial since the decrease in H<sub>2</sub> level is not statistically verified. In general, we observed H<sub>2</sub> production under light in BG11<sub>0</sub> with glucose to be less stable and reproducible compared to other conditions. The data presented for this condition in Figures 1C and 1D were collected from two individual experiments in which the variation between technical replicates was deemed acceptable.

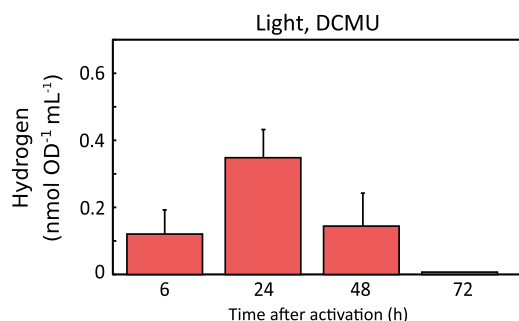


**Figure 2. *In vivo* H<sub>2</sub> production from synthetically activated *Thermoanaerobacter* HydS in *Synechocystis***

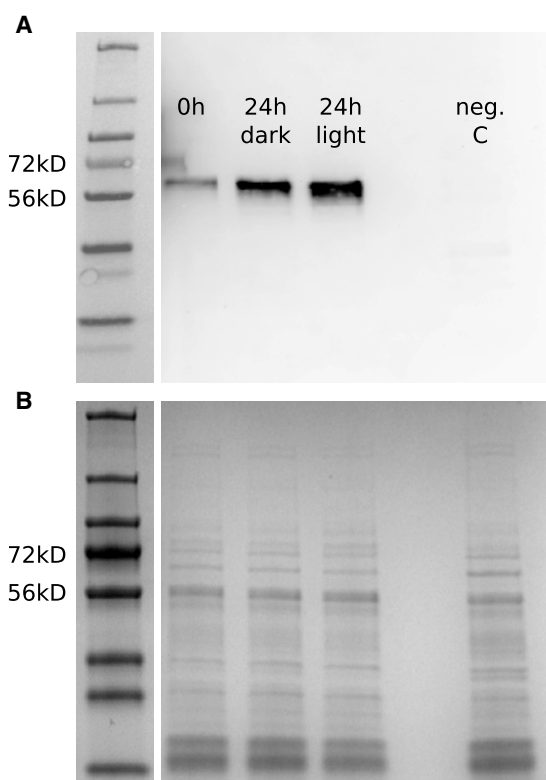
Accumulated H<sub>2</sub> by *Synechocystis* PCC 6803  $\Delta$ hox harboring a synthetically activated *Tam* HydS during light incubation with DCMU inhibition in BG11 medium.

Figure displays nanomoles of accumulated H<sub>2</sub> gas/mL culture, normalized to OD<sub>750</sub> nm. Note the scale with only very low activities. Data points represent means of 2 individual experiments, and error bars depict SDs.

Overall, dark fermentative conditions provide the best environment for H<sub>2</sub> production, and the differences in H<sub>2</sub> production between conditions are striking. The best medium composition for H<sub>2</sub> production by *Sm* HydA in darkness (BG11<sub>0</sub> without glucose) provides almost neglectable production in light with DCMU inhibition. The same dark condition (BG11<sub>0</sub> without glucose) facilitates nearly 10 times higher H<sub>2</sub> production than the best condition in light (BG11<sub>0</sub> with glucose). It is interesting to note that glucose is essential for H<sub>2</sub> production in BG11 darkness (Figures 1A and 1B), in which the production evidently is glucose dependent. In nitrate-free media, however, glucose has a negative influence on H<sub>2</sub> production and reduces the production significantly. Thus, the highest reported H<sub>2</sub> production in this work is fermentative, but not dependent on glucose. The cell cultures in BG11<sub>0</sub> without glucose have never been exposed to any external organic C sources, and all of the electrons for H<sub>2</sub> production are derived purely from photosynthetic internal substrates.

The cells expressing *Tam* HydS show very limited H<sub>2</sub> production after activation and incubation in light, and only in BG11 without glucose. This is in line with the putative sensory roll of the group D, subclass M2e enzyme. Less than 0.5 nmol H<sub>2</sub> OD<sup>-1</sup> mL<sup>-1</sup> was measured at 24 h after activation, and at 72 h, the produced H<sub>2</sub> had been consumed (Figure 2). This is the only condition in which we were able to detect any activity from *Tam* HydS when expressed in *Synechocystis*. Since the original host organism *Thermoanaerobacter mathranii* is a thermophilic bacterium, 30°C as used here, may have been too low to facilitate substantial enzyme activity. A recent *in vitro* report specifies only ~25% H<sup>+</sup> reduction activity at 30°C compared to 60°C.<sup>30</sup> Even so, the production observed here enables a direct comparison of potential differences in activity between groups and subclasses of [FeFe]-hydrogenases under our conditions.

It is intriguing that H<sub>2</sub> production from *Tam* HydS, albeit low, was observed exclusively during light incubation in BG11 without glucose, a condition in which *Sm* HydA displayed very limited production compared to, for example, in darkness with glucose (Figure 1). While in other conditions, where the group A [FeFe]-hydrogenase demonstrated a much higher H<sub>2</sub> production capacity compared to BG11 without glucose, *Tam* HydS remained seemingly inactive. The two hydrogenases display optimal *in vivo* production as far as investigated in the present study, under



**Figure 3. Expression levels of *Solobacterium HydA* in *Synechocystis* under light and dark incubation**

Representative western immunoblot analysis of *Synechocystis* PCC 6803  $\Delta$ *hox* harboring a synthetically activated *Sm HydA* under  $N_2$ -starved conditions. Samples were collected immediately after activation (0 h) or after 24 h of incubation in either darkness (24 h dark) or light with DCMU inhibition (24 h light).

Figure depicts (A) anti-Strep signal from immunoblotting targeting the Strep-tagged *Sm HydA* protein and (B) SDS-PAGE for total protein loading reference. Negative control (neg. C) is the background strain *Synechocystis*  $\Delta$ *hox*. The left-most lanes display the protein size migration reference ladder, with molecular masses corresponding to 72 and 56 kDa indicated.

vastly different circumstances, and we propose further investigations of group D [FeFe]-hydrogenases to better understand its performance and functions under diverse environmental conditions.

### High protein accumulation but low *in vivo* activity during light incubation

The condition that facilitates the highest  $H_2$  accumulation in our experiments is dark incubation in BG11<sub>0</sub> without glucose. When the same medium composition is used but cells are incubated under moderate to high irradiation ( $80 \mu\text{mol photons m}^{-2} \text{s}^{-1}$ ) with PSII inhibition, only very low levels of  $H_2$  production can be detected (Figure 1). We investigated the relative *Sm HydA* levels in the *Synechocystis*  $\Delta$ *hox SmhydA* strain after a 24-h incubation in BG11<sub>0</sub> without glucose, in either light or darkness, using protein immunoblotting targeting the C-terminal Strep-tag fused to the hydrogenase. A representative immunoblot is presented in Figure 3. Substantial protein accumulation was observed after 24 h, both in darkness and in light.

It is evident from the immunoblotting that incubation in light has no negative effect on *Sm HydA* accumulation in BG11<sub>0</sub> without glucose; in fact, the opposite appears to be the case. Thus, limited  $H_2$  accumulation in light (Figures 1C and 1D) cannot be



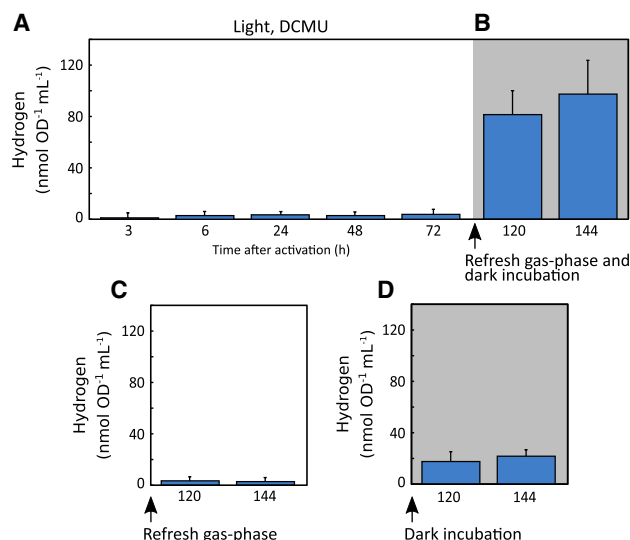


**Figure 4. In vivo H<sub>2</sub> production from synthetically activated *Solobacterium* HydA in *Synechocystis* after prolonged incubation in light**

Accumulated H<sub>2</sub> by *Synechocystis* PCC 6803  $\Delta$ hox harboring a synthetically activated *Sm* HydA under N<sub>2</sub>-starved conditions. H<sub>2</sub> accumulation was monitored during (A) initial incubation in light with DCMU inhibition in an Ar atmosphere followed by (B) restoration of the gas phase by sparging with Ar gas and transition to darkness, (C) restoration of the gas phase by sparging with Ar gas and continued incubation in light, and (D) transition to dark incubation without any gas phase restoration.

Figures display nanomoles of accumulated H<sub>2</sub> gas/mL culture, normalized to OD<sub>750</sub> nm. Data points represent means of 2–4 individual experiments, and error bars depict SDs.

due to the lack of expressed protein. However, the immunoblot does not discriminate between matured and unmaturing enzyme, and the amount of active enzyme in the different conditions cannot be deduced. The lower protein levels at the time of activation (0 h; Figure 3) can be attributed to the fact that the cells are harvested and concentrated shortly before the addition of the subcluster mimic. At this time point, cells have been dividing rapidly for several days, resulting in the continuous dilution of expressed *Sm* HydA. After harvesting, activation, and incubation in darkness or in light with DCMU inhibition, cell division rapidly stops and the heterologously expressed protein starts to accumulate.

### The semisynthetic hydrogenase is functional well beyond 72 h

To further investigate the lifetime of the *in vivo*-operating semisynthetic *Sm* HydA and to elucidate the reason for the limited production in light, we exposed *Synechocystis*  $\Delta$ hox *SmhydA* to a period of darkness after activation and a long (72 h) incubation in continuous light.

After the addition of [2Fe]<sup>adt</sup> and 72 h incubation in light (80  $\mu$ mol photons m<sup>-2</sup> s<sup>-1</sup>) with DCMU inhibition in BG11<sub>0</sub> without glucose (Figure 4A), *Synechocystis*  $\Delta$ hox *SmhydA* cultures were exposed to the following treatments: (1) sparged with Ar and moved to darkness (Figure 4B), (2) sparged with Ar but placed back under light (Figure 4C), or (3) moved to darkness without sparging (Figure 4D). During the initial 72-h light incubation, and at 48 and 72 h after treatment (120 and 144 h after incubation with [2Fe]<sup>adt</sup>), accumulated H<sub>2</sub> was measured in the sample vials (Figure 4). A distinct H<sub>2</sub> production was detected in cells sparged with Ar and transferred to darkness (Figure 4B). H<sub>2</sub> production was also recovered when kept under illumination after the sparging treatment; however, the accumulation of H<sub>2</sub> stopped at the same low levels it reached during the initial incubation (Figure 4C).



The  $H_2$  accumulation from cell cultures sparged with Ar and transferred to darkness was measured to be  $94 (\pm 33) \text{ nmol } H_2 \text{ OD}^{-1} \text{ mL}^{-1} \text{ 72 h}$  after the transfer (144 h after activation). This is less than half of the accumulated production measured at 72 h from cells in BG11<sub>0</sub> incubated in darkness directly upon activation (Figure 1B), but still remarkable considering how much time had passed since the hydrogenase was activated. The poor  $H_2$  production under light in BG11<sub>0</sub> without glucose (as seen in Figures 1 and 3) is clearly not due to any lack of functional, activated hydrogenase within the cells. Interestingly, the *Synechocystis*  $\Delta hox \Delta smhydA$  strain, harboring a heterologously expressed and artificially activated [FeFe]-hydrogenase, is capable of  $H_2$  production >72 h after the single addition of  $[2Fe]^{adt}$  at the start of the experiment. This long-lived *in vivo* activity shows that synthetic activation may prove useful not only in quick and convenient characterization experiments but also for extended  $H_2$  production applications.

Cell cultures moved to darkness without sparging with Ar after the initial 72 h light incubation (Figure 4D) displayed increased  $H_2$  production compared to cultures kept under light (Figure 4C), but with significantly lower production compared to cultures sparged with Ar before the transfer to dark incubation (Figure 4B). Many [FeFe]-hydrogenases are irreversibly inactivated by  $O_2$ ,<sup>34,35</sup> but if  $O_2$  evolution during the light incubation would be the cause of the decreased production, a similar decrease would also be expected in cells sparged before the transfer to darkness. This, together with the fact that no  $O_2$  was detected in the sample vials during or after the light incubation, allows us to exclude inactivation by  $O_2$  as the cause of the low production seen without sparging. Likewise, since  $H_2$  concentrations reached higher levels in many other experimental conditions, the accumulation of  $H_2$  and reaction back pressure can be excluded. Instead, we attribute the activity decrease to the accumulation of other gases during incubation in light. Metabolically produced volatile thiols, or carbon monoxide from decomposition of  $[2Fe]^{adt}$ , may accumulate in our closed cultivation system and inhibit the [FeFe]-hydrogenase.<sup>36,37</sup>

When examining the protein expression levels of *Sm HydA* during longer incubation in BG11<sub>0</sub> with DCMU in light, followed by sparging with Ar gas and transfer to either darkness or continued light incubation, we confirm the presence of the enzyme throughout the entire experiment (Figure 5). After 72 h incubation in light, there are significant levels of *Sm HydA* available in the cells. We know from the *in vivo* activity experiments (Figure 4) that at least a portion is functional and capable of  $H_2$  production when provided with the right conditions. Following the same trend as seen in Figure 3, Figure 5 shows that darkness incubation results in lower *Sm HydA* content compared to light, also after an initial 72-h light incubation. The fact that  $H_2$  production during darkness vastly exceeds the production in light (Figure 4), even though the protein content is lower, is interesting, especially as there is no lack of activated enzyme after 72-h light incubation (Figure 4B). This is further proof of the intimate connection between the metabolic status of the cell and the semisynthetic hydrogenase. These results, together with the inhibitor studies performed in a strain harboring *Cr HydA1*,<sup>19</sup> suggest that the limited production in light is attributable to insufficient electron donation and incompatible electron carriers. It appears as though no suitable electron donor to *Sm HydA* is available in light with DCMU inhibition in significant amounts, ruling out PSI-reduced ferredoxin as the prime redox partner. The full nature of the electron supply to the activated *Sm HydA* in darkness remains to be clarified, but a fermentatively reduced ferredoxin or NAD(P)H are suggested to be the main contributor, with the former considered most likely.

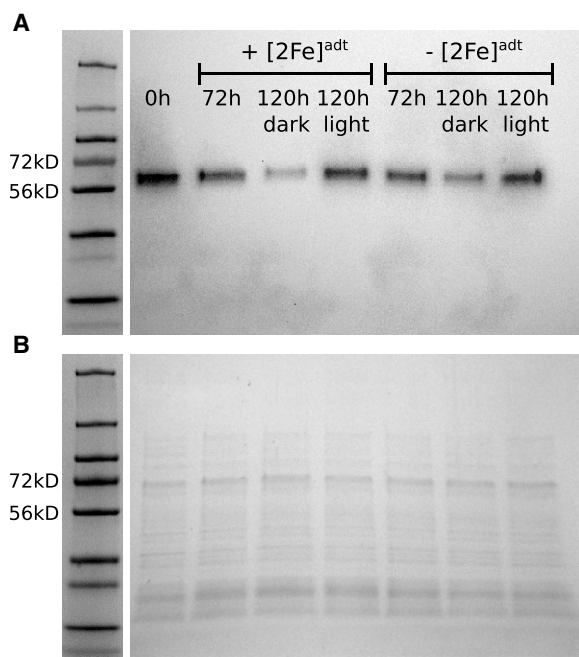


**Figure 5. Expression levels of *Solobacterium* HydA in *Synechocystis* after prolonged incubation in light**

Western immunoblot analysis of *Synechocystis*  $\Delta$ *hox* *SmhydA* under  $N_2$ -starved conditions with DCMU inhibition, with (+) or without (–) the addition of  $[2Fe]^{adt}$  at the start of the experiment (0 h). Samples were collected immediately (0 h) and after 72 h incubation in light (72 h). Thereafter, the remaining cell cultures were sparged with  $Ar$  and additional samples were collected after 48 h incubation in darkness (120 h dark) and after 48 h incubation in light (120 h light).

(A and B) Anti-Strep signal from immunoblotting targeting the Strep-tagged *Sm* HydA (A) and (B) SDS-PAGE for total protein loading reference. The left-most lanes display protein size migration reference ladder, with molecular masses corresponding to 72 and 56 kDa indicated. For corresponding *in vivo*  $H_2$  production levels, see Figures 4A–4C.

Also, as seen in Figure 5, the presence of  $[2Fe]^{adt}$  did not lead to increased or decreased *Sm* HydA levels in the examined condition, and we conclude that the incorporation of the subcluster mimic does not affect the *in vivo* stability of the enzyme in our cyanobacterial host. When comparing the relative protein levels in Figures 3 and 5, it is apparent that *Sm* HydA content at 72 h and forward, regardless of light regime, is lower than at 24 h. Since the immunoblots are developed individually, and with different total protein content loaded on the gels, band strengths are not comparable between the blots. However, the 0 h signal can be used as a crude normalization between the experiments. *Sm* HydA levels at 24 h (both in light and in dark) are higher compared to levels at the start of the experiment (Figure 3) (as discussed above), whereas levels at 72 h and forward appear slightly lower (in light) or clearly lower (in darkness) compared to levels at the start of the experiment (Figure 5). The lower protein levels during the later stages of the experiment may contribute to the lower  $H_2$  accumulation seen 48 and 72 h after the transfer to darkness following a 72-h light incubation (Figure 4B), compared to the levels observed after the same time period of dark incubation directly upon activation (Figure 1).

#### Comparison of group A [FeFe]-hydrogenases

To compare the performance of *Sm* HydA *in vivo* in *Synechocystis*  $\Delta$ *hox* to a more well-studied [FeFe]-hydrogenase, we expressed HydA1 from *Chlamydomonas reinhardtii* (*Cr* HydA1) (Table S1) in *Synechocystis*  $\Delta$ *hox* using an identical expression strategy and

genetic construct architecture to that used in *Synechocystis*  $\Delta$ hox *SmhydA* and *Synechocystis*  $\Delta$ hox *TamhydS*. The resulting strain, *Synechocystis*  $\Delta$ hox *CrhydA1*, was anaerobically incubated with 100  $\mu$ g (50  $\mu$ g/mL, 78  $\mu$ M)  $[2\text{Fe}]^{\text{adt}}$ , and  $\text{H}_2$  production was monitored in nitrate-starved conditions with and without the addition of glucose, in darkness and under light with DCMU inhibition. Comparison in darkness reveals highly similar  $\text{H}_2$  production profiles between the two strains (Figure 6A). A total of 251 ( $\pm$  17) nmol  $\text{H}_2$  OD $^{-1}$  mL $^{-1}$  was detected in the headspace of the *CrHydA1*-expressing culture at 72 h after activation, which is almost identical to the levels measured from *Synechocystis*  $\Delta$ hox *SmhydA*. This high similarity suggests an underlying restriction in electron supply to the hydrogenases as a limiting factor for the production under these conditions, rather than a protein capacity-related limitation. The equivalent observation can be made in glucose-supplemented dark condition, in which  $\text{H}_2$  accumulation also did not differ significantly between the two strains.

The same comparison, made in light under nitrate-deprived conditions with DCMU inhibition, reveals a more complex situation (Figure 6B). Without glucose supplementation to the BG11<sub>0</sub> cultivation media, *Synechocystis*  $\Delta$ hox *CrhydA1* produced only limited amounts of  $\text{H}_2$  in light with DCMU inhibition and also for a very limited time (Figure 6B). Although the production appears higher than that for the *SmHydA*-expressing strain,  $\text{H}_2$  levels are so low that we hesitate to draw conclusions regarding this. Accumulated  $\text{H}_2$  produced from *Synechocystis*  $\Delta$ hox *CrhydA1* in glucose-supplemented conditions reached 13 ( $\pm$  2) nmol  $\text{H}_2$  OD $^{-1}$  mL $^{-1}$  at 24 h after activation with  $[2\text{Fe}]^{\text{adt}}$  and did not change significantly during the rest of the experiment. The significant  $\text{H}_2$  production observed for *Synechocystis*  $\Delta$ hox *SmhydA* between 24 and 72 h was not apparent in the strain expressing *CrHydA1*. Thus, although both strains perform better under dark fermentative conditions, the decline we see in  $\text{H}_2$  production in glucose-supplemented conditions in light with DCMU inhibition is evidently less prominent for *SmHydA* than for *CrHydA1*.

The limited production observed for *Synechocystis*  $\Delta$ hox *CrhydA1* in DCMU-inhibited,  $\text{N}_2$ -deprived light conditions without glucose also agrees with results published previously for a comparable strain (expressing an untagged, truncated *CrHydA1* from a differently codon-optimized gene).<sup>19</sup> It is apparent that this condition does not facilitate any noteworthy *in vivo*  $\text{H}_2$  production in cyanobacteria from any of the two group A [FeFe]-hydrogenases investigated in the present work. The corresponding condition in darkness, however, gives the highest production of all of the tested conditions for both *Synechocystis*  $\Delta$ hox *SmhydA* and *Synechocystis*  $\Delta$ hox *CrhydA1*. We note that in both cases, no external electron sources are being provided to the cell cultures before or during the experiment. The only difference is the light regime and the addition of a PSII inhibitor (as stated above, PSII inhibition by DCMU had no impact on  $\text{H}_2$  production in darkness). The results indicate a dramatic difference in internal electron supply to the [FeFe]-hydrogenases in darkness, in which no photosynthetic electron transport is possible, compared to in light with DCMU inhibition, in which cyclic photosynthetic electron transport through PSI is still operating. When the group A, subclass M3 [FeFe]-hydrogenase from *Clostridium acetobutylicum* was expressed together with a functional biological maturation machinery in the unicellular cyanobacterium *Synechococcus elongatus* PCC 7942, a significant light-driven  $\text{H}_2$  production was observed upon PSII inhibition with DCMU.<sup>33</sup> Light-dependent production was also observed when the *C. acetobutylicum* [FeFe]-hydrogenase was inserted and biologically matured in heterocysts of the filamentous cyanobacterium *Nostoc* PCC 7120.<sup>15</sup> Interestingly, the subclass M3 *HydA* enzyme is evidently capable of light-driven  $\text{H}_2$  production in two diverse cyanobacterial strains, whereas subclass M2 *SmHydA* and subclass M1 *CrHydA1* in

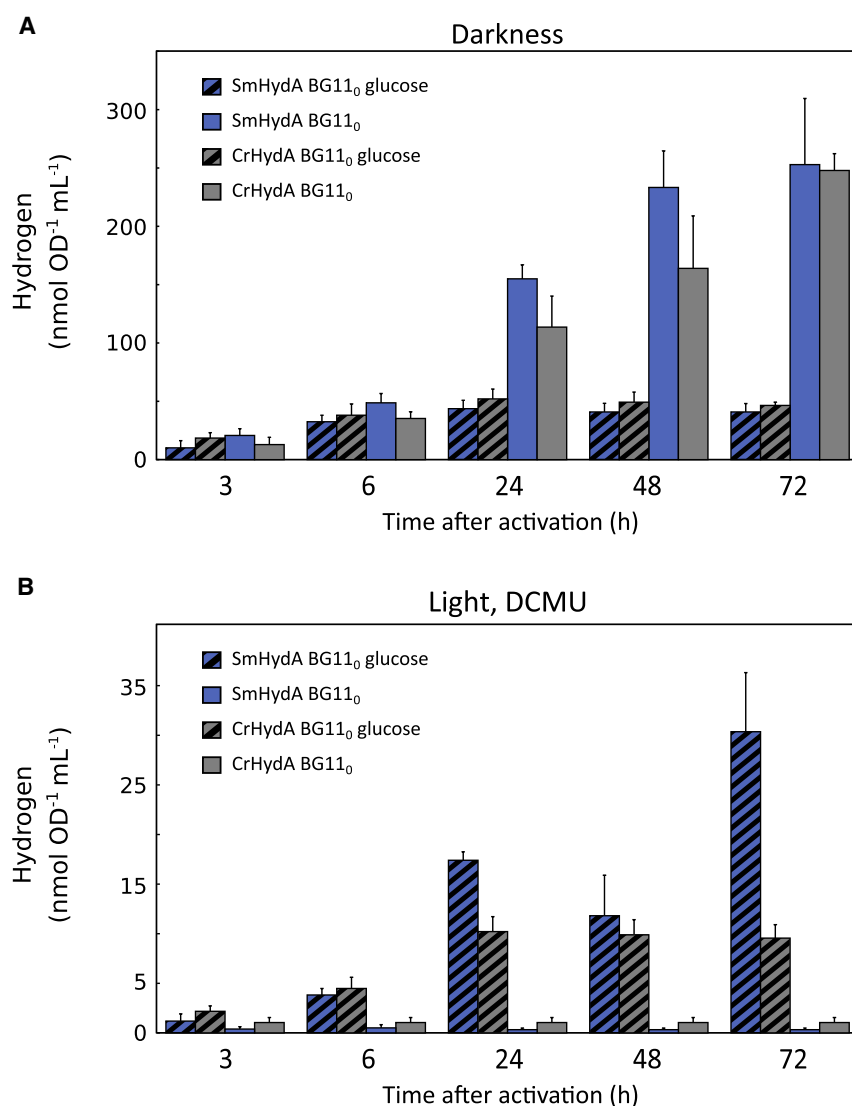


**Figure 6. Comparison of *in vivo* H<sub>2</sub> production from synthetically activated *Solobacterium* HydA and *Chlamydomonas* HydA1 in *Synechocystis***

H<sub>2</sub> production comparison between synthetically activated *Solobacterium moorei* [FeFe]-hydrogenase (Sm HydA, blue bars) and *Chlamydomonas reinhardtii* [FeFe]-hydrogenase (Cr HydA, gray bars) in living cells of *Synechocystis* PCC 6803  $\Delta hox$ . Bars represent accumulated H<sub>2</sub> in BG11<sub>0</sub> in (A) darkness and (B) light with DCMU inhibition with (black-striped bars) or without (non-striped bars) glucose.

Figures display nanomoles of accumulated H<sub>2</sub>/mL culture, normalized to OD<sub>750</sub> nm. Data points represent means of 2–4 individual experiments, and error bars depict SDs.

*Synechocystis* are not. This may be attributed to strain-specific metabolic differences or to differences in the deployed enzymes (e.g., iron-sulfur cluster composition). Both possibilities can be readily investigated using artificial maturation and present exciting questions for further research.

Artificial *in vivo* activation again proves to be an invaluable tool for [FeFe]-hydrogenase investigations. In the present study, we report the successful heterologous expression and synthetic activation of two novel [FeFe]-hydrogenases, Sm HydA from *Solobacterium moorei* and Tam HydS from *Thermoanaerobacter mathranii*,

in living cells of the unicellular cyanobacterium *Synechocystis* PCC 6803. Our work expands the number and diversity of [FeFe]-hydrogenases tested in photosynthetic microbes and provides important clues for future investigations, developments, and understanding of biological and bioinspired H<sub>2</sub> production systems.

The *Synechocystis* strain harboring the semisynthetic *Sm* HydA is capable of significant H<sub>2</sub> production under several environmental conditions. The enzyme connects to the metabolic status of the host cells and accepts intrinsic electrons from the cellular metabolism. The highest H<sub>2</sub> production was observed under N<sub>2</sub>-starved conditions, in darkness without the supply of an external C substrate. This production is fermentative, with substrate electrons derived from photosynthetically produced internal compounds. The reducing power for the produced H<sub>2</sub> is therefore derived purely from photosynthetic water splitting in an indirect fashion. Providing an external fermentation substrate did not increase the H<sub>2</sub> production under these conditions—in fact, it drastically reduced it. This is a unique behavior, not observed in fermentative H<sub>2</sub> production from heterotrophic organisms, and highlights the necessity to investigate a broad range of conditions and host organisms when developing biological H<sub>2</sub> production systems. The H<sub>2</sub> production from the semisynthetic *Sm* HydA proved to be remarkably long-lived. It was active well beyond 24 h in our initial screening, and when further investigated, we could show active hydrogenase operating *in vivo* beyond 72 h after synthetic activation. This is an astonishing lifetime for a hydrogenase-based production system with semi-artificial components, and we are confident that both stability and efficiency can be enhanced further by the optimization of the cultivation system and synthetic activation procedure.

Activation of the group D, sub-class M2e [FeFe]-hydrogenase *Tam* HydS revealed clear differences compared to the more well-studied group A [FeFe]-hydrogenases. Our results indicate that the two groups are suitable for *in vivo* H<sub>2</sub> production in cyanobacteria under vastly different environmental circumstances, possibly accepting electrons for proton reduction from different parts of the cellular metabolism. Although this clearly needs deeper investigation, especially considering the limited production from the group D enzyme, our results open up interesting co-expression systems, in which [FeFe]-hydrogenases from different groups and subclasses operate in tandem for maximized reduction power absorption and H<sub>2</sub> production efficiency.

For H<sub>2</sub> to truly become the sustainable fuel of the future, production needs to be based on water splitting by renewable energy, independent of rare earth metals. Hydrogenases operating in photosynthetic microorganisms is a promising strategy that satisfies these criteria and offers straightforward upscaling. Our results underscore the value of investigating a wide range of [FeFe]-hydrogenases in a photosynthetic environment to identify efficient candidates for future H<sub>2</sub> production systems, and *in vivo* synthetic activation offers the most direct, convenient, and reliable way to examine different engineered strains, enzymes, and cofactors in this context.

## EXPERIMENTAL PROCEDURES

### Resource availability

#### Lead contact

Further requests for procedures and resources can be directed to the lead contact, Prof. Peter Lindblad ([peter.lindblad@kemi.uu.se](mailto:peter.lindblad@kemi.uu.se)).

#### Materials availability

All of the unique materials generated in this study are available from the lead contact upon reasonable request.

### Data and code availability

All data associated with the study are available from the lead contact upon reasonable request.

### Subcluster mimic

Subcluster mimic  $[\text{Fe}_2(\text{adt})(\text{CN})_2(\text{CO})_4]^{2-}$  ( $[\text{2Fe}]^{\text{adt}}$ ,  $\text{adt} = -\text{SCH}_2\text{NHCH}_2\text{S}-$ ) was synthesized in accordance with literature protocols with minor modifications, and verified by Fourier transform infrared (FTIR) spectroscopy.<sup>38–40</sup> All of the anaerobic work was performed in an MBRAUN Labmaster glovebox under an Ar atmosphere ( $[\text{O}_2] \leq 10$  ppm).

### Strains and growth conditions

Glucose-tolerant *Synechocystis* sp. strain PCC 6803  $\Delta\text{hoxYH}$  (*Synechocystis*  $\Delta\text{hox}$ ) cells were cultivated at 30°C in BG11 media under continuous irradiance of 40  $\mu\text{mol photons m}^{-2} \text{ s}^{-1}$ . *Synechocystis*  $\Delta\text{hox Sm-hydA}$ , *Synechocystis*  $\Delta\text{hox Tam-hydA}$ , and *Synechocystis*  $\Delta\text{hox Cr-hydA}$ -engineered cells were cultivated under similar conditions, but in media supplemented with kanamycin to a final concentration of 50  $\mu\text{g mL}^{-1}$ . When necessary, combined  $\text{N}_2$  step down was carried out, after cultivation in BG11 media to  $\text{OD}_{750} = 0.8 - 1.2$ , by centrifugation at 4,500  $\times g$  for 5 min, washing 3 times in BG11<sub>0</sub> media, and suspending the cells to a final  $\text{OD}_{750} = 0.8 - 1.2$ . The combined  $\text{N}_2$ -starved cells were harvested 12–14 h after step down for further experiments.

All cloning was done using *E. coli* strain DH5 $\alpha$  Z1 grown at 37°C in Luria broth (LB) liquid medium and on plates containing LB medium solidified with 1% (w/v) agar, supplemented with 50  $\mu\text{g mL}^{-1}$  kanamycin.

### Plasmid construction and transformation

C-terminally StrepII-tagged *Tam-hydA* and *Sm-hydA* coding sequences was amplified by PCR from the corresponding template plasmid described in Land et al.<sup>21</sup> The resulting fragments were fused to a  $\text{Ptrc}_{\text{core}}$ -BCD2 expression unit<sup>19</sup> in an overlap extension PCR. Fused fragments were amplified and cloned into broad host range shuttle vector pPMQAK1<sup>41</sup> with restriction digestion (FastDigest XbaI and BclI, Thermo Fisher Scientific) and ligation (Quick Ligation Kit, New England Biolabs). The *Cr-hydA* coding sequence used in this study was codon optimized and synthesized by GenScript for a previous unpublished work. The *Cr-hydA* fragment was amplified by PCR in two subsequent reactions, as previously described,<sup>19</sup> and the resulting fragment was cloned into broad host range shuttle vector pPMQAK1 with restriction digestion (FastDigest EcoRI and BclI, Thermo Fisher Scientific) and ligation (Quick Ligation Kit, New England Biolabs). The subsequent amplifications facilitated the two-step addition of the promoter and bicistronic adaptor to the *Cr-hydA* coding sequence and introduction of a C-terminal StrepII-tag. Annotated sequences of the three genetic constructs can be seen in Table S1. Plasmids were transformed to *Synechocystis*  $\Delta\text{hox}$  by triparental mating, as described,<sup>42</sup> with *E. coli* HB101 carrying the conjugal plasmid pRL443 and the cargo plasmids carried on *E. coli* DH5 $\alpha$  Z1.

### H<sub>2</sub> production assay

A total of 20 mL culture with a cell density of  $\text{OD}_{750} = 0.8 - 1.2$  was harvested at 4,500  $\times g$ , resuspended in 2 mL fresh BG11 or BG11<sub>0</sub> supplemented with 50  $\mu\text{g mL}^{-1}$  kanamycin, and sparged with Ar for 10 min. Where necessary, the cultivation media was supplemented with 30  $\mu\text{M}$  DCMU and/or 50 mM glucose. After resuspension and sparging, cells were relocated to the glovebox and transferred to 9-mL

glass vials. *In vivo* synthetic activation with 100  $\mu\text{g}$   $[\text{2Fe}]^{\text{adt}}$  was carried out as previously described.<sup>19</sup> After sealing the sample vials with rubber septa, samples were incubated at 30°C on a rotary shaker (120 rpm) in either darkness or under 80  $\mu\text{mol photons m}^{-2} \text{ s}^{-1}$  white light. Dark samples were wrapped in Al foil and kept in a black, light-protected box on the same shaker as the light samples. Where applicable, refreshing of the gas phase was performed by sparging the sample vials with Ar for 10 min.

### **H<sub>2</sub> measurement**

H<sub>2</sub> content in sample vials was monitored by injecting 100  $\mu\text{L}$  headspace gas into a gas chromatograph (GC; PerkinElmer) equipped with a thermal conductivity detector and a stainless-steel column packed with Molecular Sieve (60/80 mesh, Sigma-Aldrich). A calibration curve was established by injecting known amounts of H<sub>2</sub>. The operational temperatures of the injection port, the oven, and the detector were 100°C, 80°C, and 100°C, respectively. Ar was used as the carrier gas at a flow rate of 35  $\text{mL min}^{-1}$ .

### **Protein extraction and Western immunoblotting**

Sample vials with synthetically activated cells of *Synechocystis*  $\Delta\text{hox Sm-hydA}$  was opened up and the 2-mL culture was immediately cooled down on ice and harvested by centrifugation, 4,000  $\times g$  for 10 min at 4°C. The pellet was washed in phosphate-buffered saline (PBS) pH 7.4, centrifuged again as above, and stored in  $-80^\circ\text{C}$ .

Cell lysis was performed by thawing the cell pellet on ice, resuspending in 800  $\mu\text{L}$  PBS with 8  $\mu\text{L}$  of 100 $\times$  Proteas Arrest (GBioscience), adding 150  $\mu\text{L}$  acid-washed glass beads, and 3  $\times$  30 s disrupting in a Precellys-24 Beadbeater (Bertin Instruments) at 5,000 rpm. Soluble protein was collected by centrifuging the cell lysate at 18,000  $\times g$  for 10 min at 4°C, transferring the supernatant to new tubes, and centrifuging again as above. Protein concentration was determined using DC protein assay (Bio-Rad). The final supernatant was collected and stored at  $-80^\circ\text{C}$ .

Total soluble protein, 3.5–5  $\mu\text{g}$ , was loaded in each lane of a Mini-PROTEAN TGX gel (Bio-Rad) and separated by SDS-PAGE. Proteins were then transferred to a Trans-Blot membrane (Bio-Rad) in a Trans-Blot Turbo membrane transfer system (Bio-Rad). Anti-Strep antibody from rabbit (Abcam) was used to detect the hydrogenase via hybridization with a secondary horseradish peroxidase (HRP)-conjugated goat anti-rabbit antibody (Bio-Rad). Interactions were detected with Clarity Western ECL Substrate (Bio-Rad), and chemiluminescence was detected in a ChemiDoc XRS system (Bio-Rad) using an exposure time of 30 s.

### **SUPPLEMENTAL INFORMATION**

Supplemental information can be found online at <https://doi.org/10.1016/j.xcrp.2021.100376>.

### **ACKNOWLEDGMENTS**

The Swedish Energy Agency (to G.B., contract no. 11674-5), the Novo Nordisk Foundation (to H.L., contract no. NNF19OC0055613), and the NordForsk NCoE program NordAqua (to P.L., project no. 82845) are gratefully acknowledged for funding. Professor Paula Tamagnini, I3S-Instituto de Investigação e Inovação em Saúde, Universidade do Porto, Porto, Portugal, is gratefully acknowledged for providing the *Synechocystis* PCC 6803  $\Delta\text{hox}$  strain. Afridi Zamader and Holly Redman, Molecular Biomimetics, Department of Chemistry-Ångström, Uppsala University, Uppsala, Sweden, are gratefully acknowledged for providing  $[\text{2Fe}]^{\text{adt}}$ .



## AUTHOR CONTRIBUTIONS

A.W. conceived the work, designed and performed all of the experiments, and wrote the first draft of the article. P.L. coordinated the project, supervised the experimental work, and extensively contributed to manuscript preparation. H.L. and G.B. provided extensive guidance on strain development and synthetic activation and contributed to manuscript preparation.

## DECLARATION OF INTERESTS

The authors declare no competing interests.

Received: October 14, 2020

Revised: December 28, 2020

Accepted: February 23, 2021

Published: March 16, 2021

## REFERENCES

- Dincer, I. (2012). Green methods for hydrogen production. *Int. J. Hydrogen Energy* 37, 1954–1971.
- Baeyens, J., Zhang, H., Nie, J., Appels, L., Dewil, R., Ansart, R., and Deng, Y. (2020). Reviewing the potential of bio-hydrogen production by fermentation. *Renew. Sustain. Energy Rev.* 131, 110023.
- Khanna, N., and Lindblad, P. (2015). Cyanobacterial hydrogenases and hydrogen metabolism revisited: recent progress and future prospects. *Int. J. Mol. Sci.* 16, 10537–10561.
- Khetkorn, W., Khanna, N., Incharoensakdi, A., and Lindblad, P. (2013). Metabolic and genetic engineering of cyanobacteria for enhanced hydrogen production. *Biofuels* 4, 535–561.
- Miao, R., Wegelius, A., Durall, C., Liang, F., Khanna, N., and Lindblad, P. (2017). Engineering cyanobacteria for biofuel production. In *Modern Topics in the Phototrophic Prokaryotes: Environmental and Applied Aspects*, P.C. Hallenbeck, ed. (Springer), pp. 351–393.
- Appel, J., Hueren, V., Boehm, M., and Gutekunst, K. (2020). Cyanobacterial *in vivo* solar hydrogen production using a photosystem I-hydrogenase (PsaD-HoxYH) fusion complex. *Nat. Energy* 5, 458–467.
- Dawood, F., Anda, M., and Shafiullah, G.M. (2020). Hydrogen production for energy: an overview. *Int. J. Hydrogen Energy* 45, 3847–3869.
- Abas, N., Kalair, E., Kalair, A., ul Hasan, Q., and Khan, N. (2020). Nature inspired artificial photosynthesis technologies for hydrogen production: Barriers and challenges. *Int. J. Hydrogen Energy* 45, 20787–20799.
- Cammack, R. (1999). Hydrogenase sophistication. *Nature* 397, 214–215.
- Birrell, J.A., Rüdiger, O., Reijerse, E.J., and Lubitz, W. (2017). Semisynthetic Hydrogenases Propel Biological Energy Research into a New Era. *Joule* 1, 61–76.
- Lubitz, W., Ogata, H., Rüdiger, O., and Reijerse, E. (2014). Hydrogenases. *Chem. Rev.* 114, 4081–4148.
- King, P.W., Posewitz, M.C., Ghirardi, M.L., and Seibert, M. (2006). Functional studies of [FeFe] hydrogenase maturation in an *Escherichia coli* biosynthetic system. *J. Bacteriol.* 188, 2163–2172.
- McGlynn, S.E., Ruebush, S.S., Naumov, A., Nagy, L.E., Dubini, A., King, P.W., Broderick, J.B., Posewitz, M.C., and Peters, J.W. (2007). *In vitro* activation of [FeFe] hydrogenase: new insights into hydrogenase maturation. *J. Biol. Inorg. Chem.* 12, 443–447.
- English, C.M., Eckert, C., Brown, K., Seibert, M., and King, P.W. (2009). Recombinant and *in vitro* expression systems for hydrogenases: new frontiers in basic and applied studies for biological and synthetic H<sub>2</sub> production. *Dalton Trans.* (45), 9970–9978.
- Avilan, L., Roumezi, B., Risoul, V., Bernard, C.S., Kpebe, A., Belhadjhassine, M., Rousset, M., Brugna, M., and Latifi, A. (2018). Phototrophic hydrogen production from a clostridial [FeFe] hydrogenase expressed in the heterocysts of the cyanobacterium *Nostoc PCC 7120*. *Appl. Microbiol. Biotechnol.* 102, 5775–5783.
- Berggren, G., Adamska, A., Lambert, C., Simmons, T.R., Esselborn, J., Atta, M., Gambarelli, S., Mouesca, J.M., Reijerse, E., Lubitz, W., et al. (2013). Biomimetic assembly and activation of [FeFe]-hydrogenases. *Nature* 499, 66–69.
- Esselborn, J., Lambert, C., Adamska-Venkates, A., Simmons, T., Berggren, G., Noth, J., Siebel, J., Hemschemeier, A., Artero, V., Reijerse, E., et al. (2013). Spontaneous activation of [FeFe]-hydrogenases by an inorganic [2Fe] active site mimic. *Nat. Chem. Biol.* 9, 607–609.
- Khanna, N., Esmieu, C., Mészáros, L.S., Lindblad, P., and Berggren, G. (2017). *In vivo* activation of an [FeFe] hydrogenase using synthetic cofactors. *Energy Environ. Sci.* 10, 1563–1567.
- Wegelius, A., Khanna, N., Esmieu, C., Barone, G.D., Pinto, F., Tamagnini, P., Berggren, G., and Lindblad, P. (2018). Generation of a functional, semisynthetic [FeFe]-hydrogenase in a photosynthetic microorganism. *Energy Environ. Sci.* 11, 3163–3167.
- Mészáros, L.S., Németh, B., Esmieu, C., Ceccaldi, P., and Berggren, G. (2018). *In Vivo* EPR Characterization of Semi-Synthetic [FeFe] Hydrogenases. *Angew. Chem. Int. Ed. Engl.* 130, 2626–2629.
- Land, H., Ceccaldi, P., Mészáros, L.S., Lorenzi, M., Redman, H.J., Senger, M., Stripp, S.T., and Berggren, G. (2019). Discovery of novel [FeFe]-hydrogenases for biocatalytic H<sub>2</sub>-production. *Chem. Sci. (Camb.)* 10, 9941–9948.
- Kageyama, A., and Benno, Y. (2000). Phylogenetic and phenotypic characterization of some *Eubacterium*-like isolates from human feces: description of *Solobacterium moorei* Gen. Nov., Sp. Nov. *Microbiol. Immunol.* 44, 223–227.
- Larsen, L., Nielsen, P., and Ahring, B.K. (1997). *Thermoanaerobacter mathranii* sp. nov., an ethanol-producing, extremely thermophilic anaerobic bacterium from a hot spring in Iceland. *Arch. Microbiol.* 168, 114–119.
- Meyer, J. (2007). [FeFe] hydrogenases and their evolution: a genomic perspective. *Cell. Mol. Life Sci.* 64, 1063–1084.
- Calusinska, M., Happe, T., Joris, B., and Wilimotte, A. (2010). The surprising diversity of clostridial hydrogenases: a comparative genomic perspective. *Microbiology (Reading)* 156, 1575–1588.
- Peters, J.W., Schut, G.J., Boyd, E.S., Mulder, D.W., Shepard, E.M., Broderick, J.B., King, P.W., and Adams, M.W.W. (2015). [FeFe]- and [NiFe]-hydrogenase diversity, mechanism, and maturation. *Biochim. Biophys. Acta* 1853, 1350–1369.
- Land, H., Senger, M., Berggren, G., and Stripp, S.T. (2020). Current State of [FeFe]-Hydrogenase Research: Biodiversity and Spectroscopic Investigations. *ACS Catal.* 10, 7069–7086.
- Van Dijk, C., Mayhew, S.G., Grande, H.J., and Veege, C. (1979). Purification and properties of

- hydrogenase from *Megasphaera elsdenii*. *Eur. J. Biochem.* **102**, 317–330.
29. Caserta, G., Adamska-Venkatesh, A., Pecqueur, L., Atta, M., Artero, V., Roy, S., Reijerse, E., Lubitz, W., and Fontecave, M. (2016). Chemical assembly of multiple metal cofactors: the heterologously expressed multidomain [FeFe]-hydrogenase from *Megasphaera elsdenii*. *Biochim. Biophys. Acta* **1857**, 1734–1740.
30. Land, H., Sekretareva, A., Huang, P., Redman, H.J., Németh, B., Polidori, N., Mészáros, L.S., Senger, M., Stripp, S.T., and Berggren, G. (2020). Characterization of a putative sensory [FeFe]-hydrogenase provides new insight into the role of the active site architecture. *Chem. Sci. (Camb.)* **11**, 12789–12801.
31. Gutthann, F., Egert, M., Marques, A., and Appel, J. (2007). Inhibition of respiration and nitrate assimilation enhances photohydrogen evolution under low oxygen concentrations in *Synechocystis* sp. PCC 6803. *Biochim. Biophys. Acta* **1767**, 161–169.
32. Hauf, W., Schlebusch, M., Hüge, J., Kopka, J., Hagemann, M., and Forchhammer, K. (2013). Metabolic Changes in *Synechocystis* PCC6803 upon Nitrogen-Starvation: Excess NADPH Sustains Polyhydroxybutyrate Accumulation. *Metabolites* **3**, 101–118.
33. Ducat, D.C., Sachdeva, G., and Silver, P.A. (2011). Rewiring hydrogenase-dependent redox circuits in cyanobacteria. *Proc. Natl. Acad. Sci. USA* **108**, 3941–3946.
34. Kubas, A., Orain, C., De Sancho, D., Saujet, L., Sensi, M., Gauquelin, C., Meynial-Salles, I., Soucaille, P., Bottin, H., Baffert, C., et al. (2017). Mechanism of O<sub>2</sub> diffusion and reduction in FeFe hydrogenases. *Nat. Chem.* **9**, 88–95.
35. Stripp, S.T., Goldet, G., Brandmayr, C., Sanganas, O., Vincent, K.A., Haumann, M., Armstrong, F.A., and Happe, T. (2009). How oxygen attacks [FeFe] hydrogenases from photosynthetic organisms. *Proc. Natl. Acad. Sci. USA* **106**, 17331–17336.
36. Roseboom, W., De Lacey, A.L., Fernandez, V.M., Hatchikian, E.C., and Albracht, S.P.J. (2006). The active site of the [FeFe]-hydrogenase from *Desulfovibrio desulfuricans*. II. Redox properties, light sensitivity and CO-ligand exchange as observed by infrared spectroscopy. *J. Biol. Inorg. Chem.* **11**, 102–118.
37. Rodríguez-Maciá, P., Reijerse, E.J., van Gastel, M., DeBeer, S., Lubitz, W., Rüdiger, O., and Birrell, J.A. (2018). Sulfide Protects [FeFe] Hydrogenases From O<sub>2</sub>. *J. Am. Chem. Soc.* **140**, 9346–9350.
38. Li, H., and Rauchfuss, T.B. (2002). Iron carbonyl sulfides, formaldehyde, and amines condense to give the proposed azadithiolate cofactor of the Fe-only hydrogenases. *J. Am. Chem. Soc.* **124**, 726–727.
39. Siebel, J.F., Adamska-Venkatesh, A., Weber, K., Rumpel, S., Reijerse, E., and Lubitz, W. (2015). Hybrid [FeFe]-hydrogenases with modified active sites show remarkable residual enzymatic activity. *Biochemistry* **54**, 1474–1483.
40. Esmieu, C., and Berggren, G. (2016). Characterization of a monocyanoide model of FeFe hydrogenases - highlighting the importance of the bridgehead nitrogen for catalysis. *Dalton Trans.* **45**, 19242–19248.
41. Huang, H.H., Camsund, D., Lindblad, P., and Heidorn, T. (2010). Design and characterization of molecular tools for a Synthetic Biology approach towards developing cyanobacterial biotechnology. *Nucleic Acids Res.* **38**, 2577–2593.
42. Heidorn, T., Camsund, D., Huang, H.H., Lindberg, P., Oliveira, P., Stensjö, K., and Lindblad, P. (2011). Synthetic biology in cyanobacteria engineering and analyzing novel functions. *Methods Enzymol.* **497**, 539–579.